JOURNAL OF CATALYSIS **169,** 103–113 (1997)
ARTICLE NO. CA971682

Hydroconversion of Methylcyclohexane on Bifunctional Sulfated Zirconia-Supported Platinum Catalysts

François Figueras,*,[1] Bernard Coq,*,[2] Christian Walter,* and Jean-Yves Carriat†

*Laboratoire de Matériaux Catalytiques et Catalyse en Chimie Organique, UMR 5618 du CNRS, ENSCM, 8 Rue de l'Ecole Normale, 34053 Montpellier Cedex, France; and †Centre de Recherche Total Raffinage et Distribution, B.P. 27, 76700 Harfleur, France

Received April 22, 1996; revised February 11, 1997; accepted February 28, 1997

A series of bifunctional catalysts prepared from sulfated zirconias (SZs) by deposition of platinum were studied in the conversion of methylcyclohexane (MCH). The main reaction observed is the isomerization to alkylcyclopentanes (ACPs), the slow step of which is the acid-catalyzed contraction of the ring. The positive order with respect to hydrogen pressure is tentatively assigned either to a nonclassical bifunctional mechanism where hydride transfer steps play a key role or to the increased formation of active Brønsted sites, coming from the reduction of Lewis sites by hydrogen. Some ring-opening products, i.e., C_7 alkanes, which represent $\geq$5% at high hydrogen pressure, are formed from ACPs either by hydrogenolysis on the Pt sites or more probably by bifunctional acid catalysis. The acidity of the samples was studied by diffuse reflectance infrared Fourier transform (DRIFT) spectroscopy and temperature-programmed desorption (TPD) of acetonitrile. Acetonitrile desorbs as two peaks, one around 410 K found on all the samples and a second at 670 K on SZ and at 500 to 570 K on Pt/SZ. Hence the introduction of Pt changes the distribution of acidity of the support. This modification is more important when chloroplatinic acid is used as precursor rather than Pt acetylacetonate. A rough correlation exists between the rate of MCH conversion on Pt/SZ and the amount of acetonitrile desorbed under the high-temperature peak. Pt/SZ catalysts doped with Fe and Mn show activities for MCH conversion close to those of unpromoted sulfated zirconias. This result can be interpreted using classical mechanisms through the charge transfer complex assumed in homogeneous catalysis.

INTRODUCTION

Sulfated zirconias (denoted in this paper as SZs) have been investigated mainly as catalysts for the acid-catalyzed isomerization of light alkanes at relatively low temperatures (1–7). The most active catalyst in this family is sulfated zirconia doped with Fe and Mn oxides, which is able to catalyze the isomerization of *n*-butane just above room temperature (8–10). The observation of cracking of neopentane as a primary reaction on this catalyst supported the proposal of super-acid properties since neopentane protonation requires a pentacoordinated carbonium ion (11). The kinetics of butane isomerization (12) and the disproportionation of propane to butanes and pentanes (13) also suggested protonation at low temperature. From labeling experiments, Sommer *et al.* (14) proposed a monomolecular mechanism for the *n*-butane isomerization on SZ, but a bimolecular mechanism was claimed on Fe, Mn–SZ (15) and Pt/SZ (16). Hence the detailed mechanism of this reaction remains a matter of discussion.

It is well known that traces of olefins accelerate acid-catalyzed conversions of hydrocarbons (17) and that such a catalysis usually results in rapid deactivation. More stable catalytic activity for the isomerization of paraffins is achieved by bifunctional catalysis, i.e., the association of a hydrogenation function with a solid acid (18–21). In this case the amount of olefins is controlled by the hydrogenation/dehydrogenation equilibrium. An interesting reaction in this context is the conversion of methylcyclohexane (MCH). This reaction has been investigated in superacids (22) and on bifunctional catalysts (23) and is considered a simple monomolecular reaction in which the slow step is the ring contraction to alkylcyclopentanes (ACPs). Moreover, the ring opening of ACPs to C_7 alkanes could constitute a model reaction for the hydrodecyclization of polynuclear condensed naphthenes, with the aim of increasing the cetane index of gas oil.

The acidity of sulfated zirconia has now been investigated by several groups (24–29), but that of the bifunctional catalyst has not yet been reported. In this case there are indications (20, 29) that the acidity shifts from Lewis to Brønsted by treatment under hydrogen, and it is questionable to relate the acidity of the support to the catalytic properties of the bifunctional catalyst. The acidity of SZ has been studied previously using the adsorption of benzene, CO, H_2, CH_4, and olefins (28). The acid strength SZ was found to be comparable to that of H-ZSM5, i.e., strong acidity but not really superacidity. Acetonitrile is a much stronger base,

[1] Present address: Institut de Recherches sur la Catalyse du CNRS, associé à l'Université C. Bernard, 2 Avenue A. Einstein, 69626 Villeurbanne Cedex, France.

[2] To whom correspondence should be addressed.

0021-9517/97 $25.00

well adapted for the measurement of the number of acid sites, and was used here to investigate the acid properties. It was therefore the aim of this work to study the acid properties of Pt/SZ by means of acetonitrile adsorption/desorption monitored by diffuse reflectance infrared Fourier transform (DRIFT) spectroscopy and temperature-programmed desorption (TPD). The dependence of acid properties as a function of the S and Pt content, the thermal treatments, and the protocol for introducing Pt will be correlated with the catalytic properties in the hydroconversion of MCH.

EXPERIMENTAL

Reactants

Zirconyl chloride ($ZrOCl_2 \cdot 8H_2O$, Fluka, purity >99.0%), ammonia (Prolabo, 28–30% NH_3), and H_2SO_4 (SDS, H_2SO_4 94–96%) were used to prepare the SZ. A commercial SZ sample (donated by MEL Chemicals, reference: XZ0707.04), calcined at 873 K, was also used as support; it will be designated ZrOY3.8S in the following. The Pt precursor was either H_2PtCl_6 (Interchim) or Pt acetylacetonate [$Pt(acac)_2$, Aldrich]. CH_3CN (Aldrich, purity >99%) and CD_3CN (Aldrich, 99.95% D) were used for TPD and infrared experiments, respectively.

Catalysts

SZ. Zirconium hydroxide was prepared by hydrolysis of $ZrOCl_2$ with concentrated ammonia. The reactants were added dropwise within 3 h and the pH was kept constant at 10. The gel was allowed to mature for 6 h before filtration and washing until the pH was 7 and no more chloride was detected in the washing solution. Two batches of $Zr(OH)_4$ were prepared and are denoted as ZrOX and ZrOZ, respectively. Sulfated $Zr(OH)_4$ was obtained by treating the zirconium hydroxide with sulfuric acid solutions of various concentrations (15 ml of solution per gram of support). The support was immersed in the sulfation solution for 5 h, then filtered and dried at 393 K.

Pt–SZ. The Pt catalysts were prepared by dry impregnation of SZ, either with an aqueous solution of H_2PtCl_6 or with a toluene solution of $Pt(acac)_2$. After contacting for 3 h, the solution was evaporated and the solid dried at 393 K. The samples were then submitted to calcination at different temperatures (Table 1) and reduced at 523 K under diluted H_2 (H_2/N_2: 20/80; ramp: 1 K min^{-1}) for 3 h. In a previous study, dealing with the state of Pt in these Pt/SZ catalysts, we have shown, by temperature-programmed reduction experiments (5 K min^{-1}), that the faster reduction rate of Pt occurred at 500 K, and that the reduction of sulfate species started at 550–570 K (30). A reduction temperature of 523 K was therefore chosen for these catalysts.

Fe,Mn–SZ. Sulfated zirconias doped with Fe and Mn were obtained by the former procedure, adding Fe^{3+} and Mn^{2+} nitrates to the solution of zirconyl chloride. Two samples were thus prepared, containing 1% Pt and either 1.1% Fe (1PtZrOS–Fe) or 0.8% Fe and 0.3% Mn (1PtZrOS–Fe,Mn). They were used for the catalytic test after calcination in air at 873 K and the standard reduction procedure.

TABLE 1

Surface Area (S_{BET}) and Chemical Composition of Sulfated Zirconia-Supported Pt Catalysts after Calcination at 673 K and Reduction at 473 K

Catalyst	S_{BET} ($m^2\ g^{-1}$)	S (wt%)	Pt (wt%)	H/Pt
1PtZrOX0.3S[a,b]	150	0.30	0.96	—
1PtZrOX2.7S[a,b]	160	2.65	1.00	0.51
1PtZrOX4.6S[a,b]	125	4.65	0.94	—
0.3PtZrOX2.7S[a,b]	160	2.73	0.34	0.39
1.7PtZrOX2.7S[a,b]	160	2.74	1.74	0.49
ZrOY3.8S	125	3.8	0	—
1.2PtZrOY3.8S[a,b]	125	3.5	1.10	0.31
1.7PtZrOY3.8S[b,c]	125	2.9	1.70	0.25
1.5PtZrOZ2.6SA[a,d]	270	2.60	1.45	0.65
1.5PtZrOZ2.6SB[a,b]	270	2.55	1.50	0.59
1.5PtZrOZ2.6SC[a,e]	135	2.20	1.50	0.03
1PtZrOS–Fe[a,e]	110	2.80	0.85	—
1PtZrOS–Fe,Mn[a,e]	110	2.20	0.84	—

[a] From H_2PtCl_6.
[b] Calcined at 673 K.
[c] From $Pt(acac)_2$.
[d] Calcined at 573 K.
[e] Calcined at 823 K.

Pt/NaHY. Pt/NaHY (Si/Al = 2.5) was prepared by competitive ion exchange between $Pt(NH_3)_4^{2+}$ and NH_4^+ for a purpose of comparison. After calcination at 773 K and reduction at 593 K, the final catalyst contained 0.5% Pt and 1.4% Na, with H/Pt ≈ 1.

Characterization

Chemical analyses of the samples were performed at the Service Central d'Analyse du CNRS (Solaize, France); for the Pt/SZ catalysts, they were determined on the activated samples, after calcination and reduction at the chosen temperatures. Surface areas and pore size distributions of the solids were determined by N_2 sorption at 77 K using a Micromeritics ASAP 2000 apparatus.

H_2 chemisorption was carried out in a conventional static apparatus. The sample was reactivated under H_2 at 523 K overnight, outgassed at 523 K for 2 h at a pressure of 2×10^{-4} Pa. A first isotherm was determined in the range 0–20 kPa. A back isotherm was then determined after evacuation at room temperature of the sample for 30 min at 2×10^{-4} Pa. H_2 uptake was estimated by the extrapolation to zero pressure of the linear part of the isotherms. The first isotherm gives the total amount of chemisorbed

hydrogen (H_{tot}), the second isotherm gives the reversible part of chemisorbed hydrogen (H_{rev}), and the difference between the two isotherms gives the irreversible part of chemisorbed hydrogen (H_{irr}).

The acid properties of the samples were studied by TPD of CH_3CN and infrared spectroscopy of CD_3CN. For TPD experiments, an aliquot of the catalyst (≈100 mg) was reactivated *in situ* under air at 673 K and subsequently reduced at 523 K in diluted H_2. After saturation of the sample with CH_3CN at room temperature, the weakly adsorbed CH_3CN was removed by outgassing under N_2 at 363 K. The CH_3CN desorption was then started under nitrogen flow (50 cm^3 min^{-1}) from 363 to 773 K at 5 K min^{-1}. The identification and quantification of CH_3CN released in the outflowing gas are performed by sampling on line every minute to a gas chromatograph.

The DRIFT spectroscopy of adsorbed CD_3CN was carried out using a Bio-Rad FTS-40 Fourier transform infrared instrument equipped with diffuse reflectance optics and environmental cell (Spectratech Ltd.) (31), with a resolution of 4 cm^{-1}. The catalyst (≈150 mg) was first treated at 473 K under He of high purity and was further passed through molecular sieves, deoxo units, and copper and charcoal traps. The sample was then treated under H_2 for 30 min at 473 K and outgassed under He flow for 2 h at the same temperature. After cooling to room temperature, amounts of 0.1 μmol of CD_3CN were pulsed to the sample until saturation through a sampling loop flushed with He. Spectra were recorded at room temperature, (i) after the first pulse (low CD_3CN coverage), (ii) after saturation and outgassing at room temperature, and (iii) after outgassing for 1 h at 373 K.

The main characteristics of the catalysts are given in Table 1.

Catalytic Tests

The reaction of MCH with H_2 was studied mainly in a dynamic glass reactor operating at atmospheric pressure. The pressures of the reactants were generally $P(\mathrm{MCH}) = 1.2$ kPa and $P(H_2) = 98.9$ kPa. The effluents were analyzed by sampling on-line to a FID gas chromatograph equipped with a J&W capillary column (60 m × 0.5 mm i.d., DB1 apolar bonded phase). An aliquot of the catalyst, typically 100 mg, was calcined and reduced *in situ* under the conditions described above. The catalytic tests were performed between 350 and 540 K with a heating rate of 0.5 K min^{-1}.

Some additional experiments were carried out in a scaled-up apparatus operating under high hydrogen pressure (≤5.5 MPa). The analyses of the gaseous and liquid effluents were performed off-line. Catalytic tests were carried out under isothermal conditions between 470 and 540 K. The same general protocol was followed for the activation of the sample except for the amount of catalyst, which was around 10–15 g.

The following parameters were evaluated:

$$\text{conversion (mol\%)} = \left(\sum_1^n (i/n)C_i\right) \Big/ \left(C_n^0 + \sum_1^n (i/n)C_i\right) \times 100.$$

$$\text{selectivity } S_i \text{ to compund } i,\ S_i \text{ (mol\%)} = C_i \Big/ \left(\sum_1^n C_i\right) \times 100,$$

where C_i is the mole percent of product with i carbon atoms and C_n^0 is the mole percent in the feed of MCH.

RESULTS

The hydroconversion of MCH produces mainly ACPs at low temperature (<500 K) and toluene at temperatures higher than 550 K for thermodynamic reasons. Trace amounts of ring-opening products (ROPs) comprising mainly *n*-heptane (*n*C7) and 2-methylhexane (2MH) are found. With our GC column, 3-methylhexane (3MH) could not be separated from 1,1-dimethylcyclopentane (1,1-dMCP). Therefore, it was not accounted for with ROPs; however, for kinetic reasons its concentration would be comparable to that of 2MH.

Influence of the Sulfur Content

$Zr(OH)_4$ (ZrOX sample) was treated with H_2SO_4 solutions of concentrations of 0.005, 0.05, and 0.5 mol $liter^{-1}$. After drying, impregnation with H_2PtCl_6, calcination at 673 K, and reduction at 523 K, the samples contained 0.3, 2.7, and 4.6 wt% S, and 1 wt% Pt (Table 1). As expected, the catalyst with the highest S content (1PtZrOX4.6S) is the most reactive at low temperature (Fig. 1a). The ACP yield leveled at around 25–30% (Fig. 1b), and ROP selectivity did not exceed 0.5% (Fig. 1c). Under the same conditions, the Pt/NaHY catalyst exhibited an activity similar to that of 1PtZrOX2.7S (Fig. 1a).

The desorption of CH_3CN (Fig. 2) showed merely two peaks at around 400–420 K (LT) and 550–600 K (HT). The total amount of CH_3CN desorbed was maximum for 2.7 wt% S, then decreased (Table 2). The proportion of CH_3CN desorbed at HT increased from 15 to 40% when the S content increased from 0.3 to 4.6 wt%.

Influence of Platinum on Activity and Acidity

The effect of Pt content was studied first, followed by the mode for introducing Pt, either from an aqueous solution of H_2PtCl_6 or from a toluene solution of $Pt(acac)_2$.

Pt contents from 0.3 to 1.7 wt% were introduced from H_2PtCl_6 on $Zr(OH)_4$ precursor (ZrOX2.7S sample). After

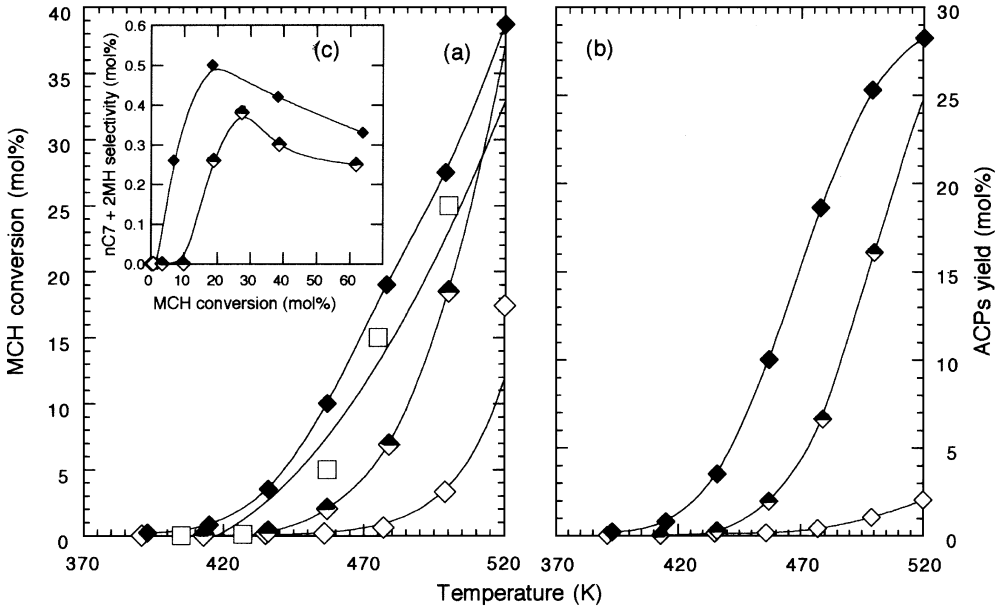

FIG. 1. Conversion of MCH over Pt/NaHY (□), and sulfated zirconia-based catalysts with different S contents: (◇) 1PtZrOX0.3S, (◓) 1PtZrOX2.7S, (◆) 1PtZrOX4.6S. (a) MCH conversion, (b) ACP yield, (c) selectivity for $nC_7 + 2MH$.

calcination at 673 K and reduction at 523 K the Pt accessibility was determined and ranged from 0.4 to 0.5 (Table 1). In the range investigated there was no effect of Pt content on MCH conversion; it remained the same. By contrast, the Pt content affected ROP selectivity, which increased with the accessible surface of Pt (Fig. 3).

There is a clear influence on MCH conversion of the protocol followed to introduce Pt. On the one hand, Pt is introduced through $Pt(acac)_2$ in toluene solution on the ZrOY3.8S sample precalcined at 823 K; thereupon the solid is calcined again at 673 K and reduced at 523 K (1.7PtZrOY3.8S sample). On the other hand, Pt is introduced through an aqueous solution of H_2PtCl_6 and activated in the same way (1.2PtZrOY3.8S sample). It turns out that the 1.7PtZrOY3.8S sample is more active than the 1.2PtZrOY3.8S sample (Fig. 4a). This behavior is very likely to be related to a higher acid strength for which there is evidence from TPD of CH_3CN (Fig. 4b). On the $Pt(acac)_2$-based catalyst, there is a shift by 80 K to higher temperature of the HT peak which corresponds to a different distribution in strength of the acid sites, since the LT peak is smaller than on the 1.2PtZrOY3.8S sample. Otherwise, the total amounts of CH_3CN desorbed are very close on the two samples (Table 2). Finally, it should be pointed out

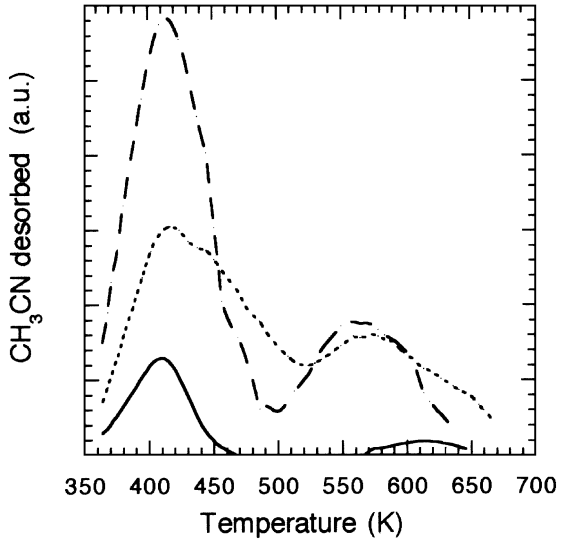

FIG. 2. TPD profiles of acetonitrile from catalysts with various S contents: (—) 1PtZrOX0.3S, (- - -) 1PtZrOX2.7S, (· · ·) 1PtZrOX4.6S.

TABLE 2

Acetonitrile Desorbed during TPD Experiments: Total Amount Q_{CH_3CN}, Amount Referred to the Sulfur Content of the Sample Q_{CH_3CN}/Q_S, and Fraction Desorbed under the High-Temperature Peak $(Q_{CH_3CN})_{HT}$

Catalyst	Q_{CH_3CN} (μmol g^{-1})	Q_{CH_3CN}/Q_S (mol/mol)	$(Q_{CH_3CN})_{HT}$ (%)
1PtZrOX0.3S	14	0.12	15
1PtZrOX2.7S	91	0.11	30
1PtZrOX4.6S	84	0.05	45
ZrOY3.8S	210	0.18	55
1.2PtZrOY3.8S	143	0.12	53
1.7PtZrOY3.8S	133	0.11	59
1.5PtZrOZ2.6SB	143	0.18	32
1.5PtZrOZ2.6SC	153	0.18	62

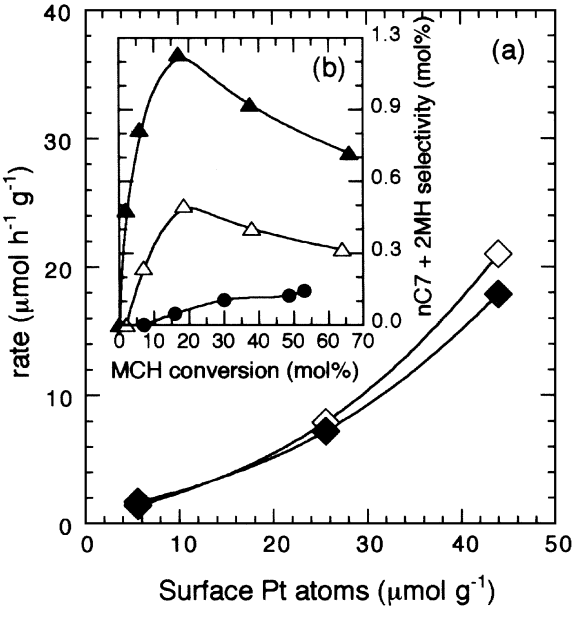

FIG. 3. (a) Formation rate of nC_7 (◇) and 2MH (◆) as a function of the concentration of surface Pt atoms for the Pt/SZ based on the ZrOX2.7S sulfated zirconia. (b) Selectivity for nC_7 and 2MH as a function of MCH conversion, for the three different samples containing 0.3% Pt (●), 1% Pt (△), and 1.7% Pt (▲).

that on Pt introduction on ZrOY3.8S, the high-temperature desorption peak of CH_3CN is shifted to lower temperature (Fig. 4b); however, the extent of this shift is lower when Pt is introduced as $Pt(acac)_2$ in organic solution than as H_2PtCl_6 in aqueous solution.

Influence of Thermal Treatments

The influence on catalytic properties of thermal treatments was studied on 1.5PtZrOZ2.6S for three calcination temperatures. Table 1 shows that the accessibility decreases sharply after calcination at 823 K and reduction at 523 K. Studying similar catalysts by TEM, H_2 chemisorption, and DRIFT spectroscopy of adsorbed CO, we have previously shown that this decrease in Pt accessibility is due mainly to poisoning by sulfur and, to a much lesser extent, by sintering of Pt particles, whose size increased from 1.2 to 3.2 nm (30).

As expected, the catalyst calcined at 823 K is the most active at low temperature, but this behavior is not maintained at temperatures higher than 480 K (Fig. 5a). Above 500 K, however, the main reaction is the dehydrogenation of MCH to toluene. The lower reactivity of the sample calcined at 823 K is therefore probably due to the very low accessibility at the Pt surface. In contrast, the higher activity, at low temperature, of the sample calcined at 823 K can

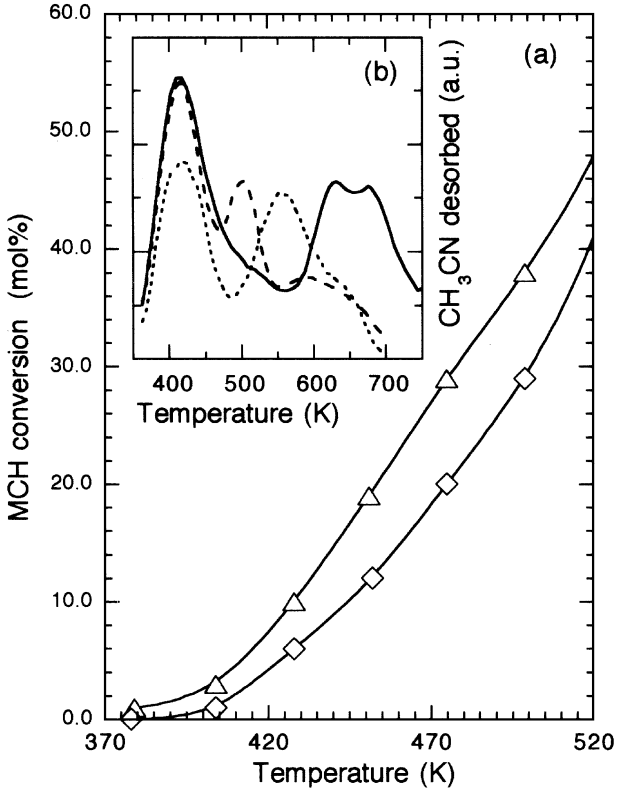

FIG. 4. (a) MCH conversion as a function of temperature. (b) TPD profiles of acetonitrile. Catalysts: (—) ZrOY3.8S, (- - -) 1.2PtZrOY3.8S, (· · ·) 1.7PtZrOY3.8S.

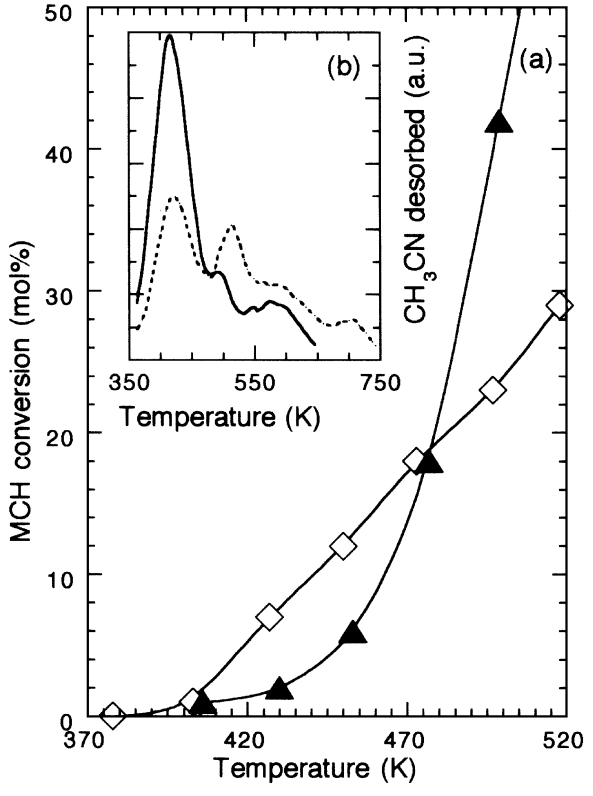

FIG. 5. (a) MCH conversion as a function of temperature. (b) TPD profiles of acetonitrile. Catalysts: 1.5PtZrOZ2.6S calcined either at 673 K (—), or at 823 K (· · ·).

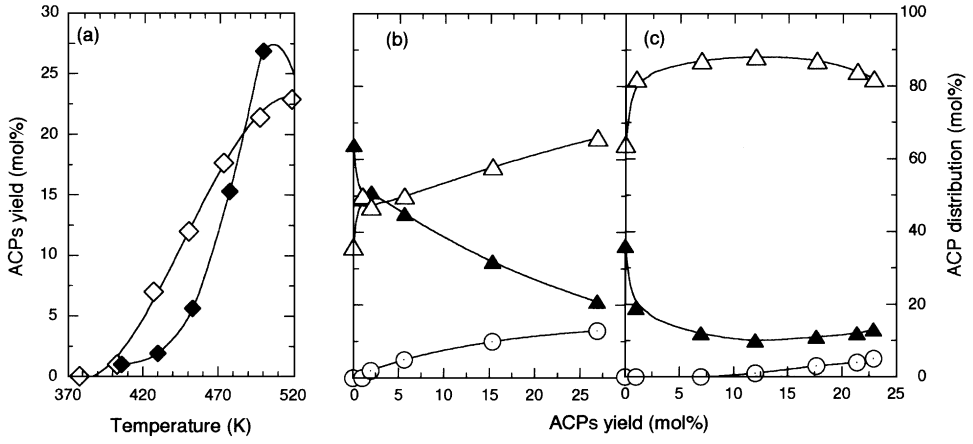

FIG. 6. (a) ACPs yield as a function of temperature for MCH conversion over 1.5PtZrOZ2.6S calcined either at 673 K (◆) or at 823 K (◇). (b, c) Product distribution between ACPs as a function of ACP yield over 1.5PtZrOZ2.6S calcined either at 673 K (b) or at 823 K (c). (▲) ECP, (△) 1,2-dMCP + 1,3-dMCP, (⊙) 1,1-dMCP.

be related to the change in acid site distribution shown by TPD of CH_3CN (Fig. 5b). A noticeable fraction of sites of weak acidity are converted into sites of higher acid strength (Table 2). The ACP yield follows the same trend as discussed previously and passes through a maximum of 25–30% at around 500 K (Fig. 6a). The distribution between the ACPs is different depending on the calcination temperature (Figs. 6b, c). At 500 K (≈25% MCH conversion) the thermodynamic distribution between ECP/(ethylcyclopentane), 1,2- plus 1,3-dMCP, and 1,1-dMCP is 11.4, 72.5, and 17.1 mol%, respectively (23). The differences observed for ACP distribution are not due to shape selectivity as proposed for Pt/H-ZSM5 (23), but are more likely to be related to the differences in acidity. Finally, ROP selectivity is very low on the sample calcined at high temperature.

Effect of Fe and Mn Promotion

The hydroconversion of MCH has been studied over Pt/SZ promoted by Fe and Mn (Fig. 7). It emerges that the addition of Fe as a simple dopant has a small negative effect on the activity, but the simultaneous addition of Fe and Mn shows a small positive effect. The rate is increased by a factor of 2, which remains much smaller than that reported by Hsu *et al.* (9) for the isomerization, in the absence of hydrogen, of *n*-butane over Fe- and Mn-containing sulfated zirconia.

Kinetic Study

The dependence of the MCH reaction rate on hydrogen pressure was examined on 0.3PtZrOX2.7S in a bench scale reactor using 15 g of sample. An almost linear increase in rate with $P(H_2)$ occurs in all the range studied (0.1–2.5 MPa) (Fig. 8). These kinetics differ significantly

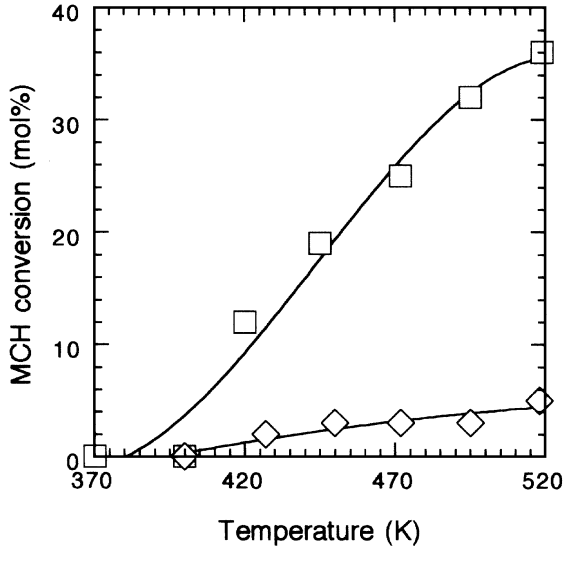

FIG. 7. MCH conversion as a function of temperature on 1PtZrOS–Fe (◇), and 1PtZrOS–Fe,Mn (□).

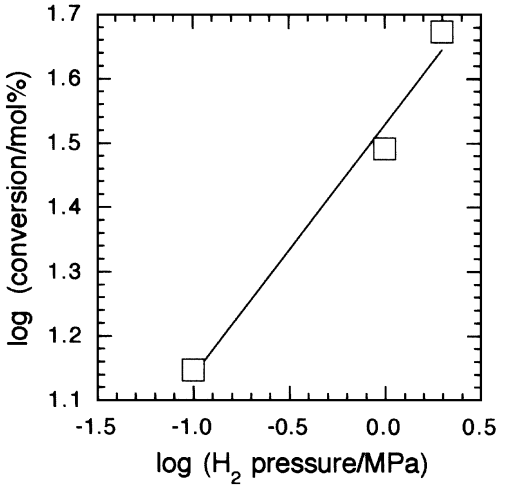

FIG. 8. MCH hydroconversion rate as a function of H_2 pressure on 0.3PtZrOX2.7S.

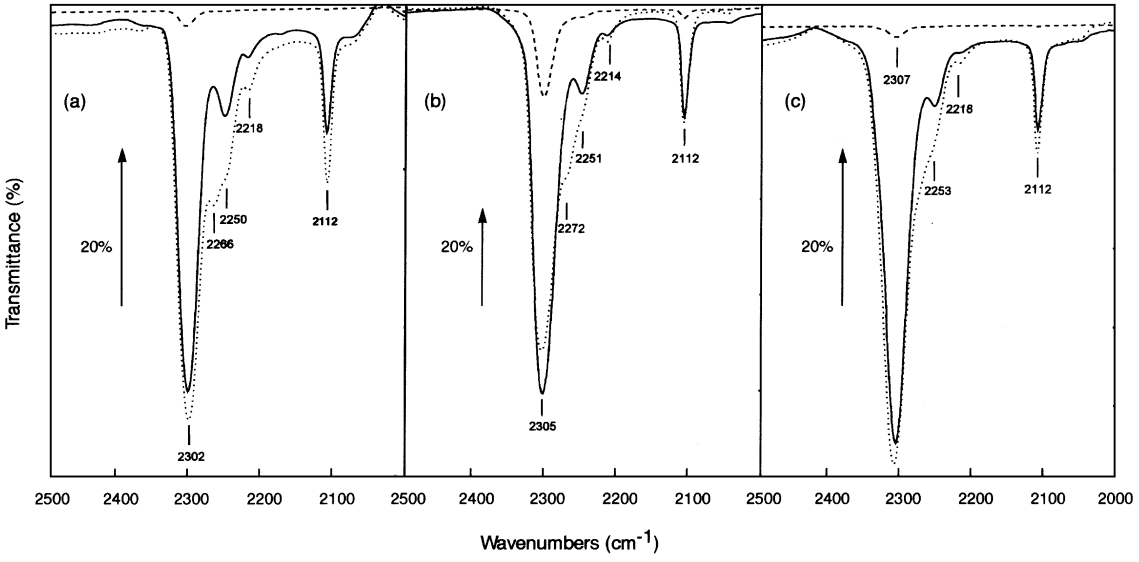

FIG. 9. Difference DRIFT spectra, in the C≡N vibration spectral region, expressing the difference between after and before adsorption of CD_3CN on different catalysts: (a) 1PtZrOX0.3S, (b) 1.5PtZrOZ2.6SB, (c) 1.2PtZrOY3.8S. (- - -) At low coverage, (· · ·) after saturation and desorption at room temperature, (—) after desorption at 373 K.

from those observed for the hydroconversion of alkanes on conventional bifunctional catalysts where a negative order with respect to hydrogen is found (32); this is in agreement with the proposed rate law assuming equilibration of hydrogenating/dehydrogenation steps on metal sites and the acid-catalyzed rearrangement of carbocations as the determining step (33). However, positive orders with respect to H_2 pressure were reported previously on Pt/SZ for conversions of *n*-heptane (21) and light alkanes (20).

DRIFT Spectroscopy

Three different samples obtained by impregnation of SZ with H_2PtCl_6 were investigated by DRIFT spectroscopy after adsorption of CD_3CN. The spectra are reported in Figs. 9–11, as differences between the spectra obtained after and before adsorption of the probe. The spectral range corresponding to C≡N, S=O, and O−H stretching vibrations have been selected. From Fig. 9 it appears that the interaction of acetonitrile with the surface is strong. The bands at 2112, 2218, and 2250 cm^{-1} are due to C−D vibration modes, while C≡N stretching frequency is expected at 2300 cm^{-1} (34–37). This band is shifted to higher frequencies on interaction with Lewis sites, and the magnitude of this shift is related to the acid strength of the Lewis sites (34). Only small differences are observed between the three samples, and the ν_{CN} is very close to the value reported by Adeeva *et al.* (37) for CD_3CN adsorbed on SZ or Fe,Mn–SZ.

On adsorption of CD_3CN, OH groups observed at 3650–3646 cm^{-1} disappear from the spectrum and a broad band appears at 3390 or 3324 cm^{-1} (Fig. 10). This corresponds to the shift of weakly acidic OH by H bonding. The different shifts of these hydroxyls are indicative of different acid strengths of the samples. The vibrations of sulfates are observed at different frequencies depending on the sample, and exhibit different shifts on acetonitrile adsorption (Table 3 and Fig. 11).

DISCUSSION

Besides the metal-catalyzed aromatization of MCH to toluene, the conversion of MCH with H_2 on Pt/SZ leads to two classes of products:

1. ACPs, formed by isomerization of MCH through a bifunctional mechanism, the rate of which is independent of the Pt surface area and is then limited by the acid function. A classical bifunctional mechanism is questionable, however, due to the positive order with respect to hydrogen pressure (Fig. 8). From similar observations for *n*-heptane hydroconversion on Pt/SZ, Iglesia *et al.* (21) proposed that

TABLE 3

Stretching Frequency Vibrations of Hydroxyl, Sulfate, and Nitrile Groups on Acetonitrile Adsorption on Three Different Catalysts

	Frequency of vibration (cm^{-1})						
	Before adsorption		After adsorption of CD_3CN				
Catalyst	ν_{O-H}	$\nu_{S=O}$	ν_{O-H}	$\nu_{S=O}$	$\nu_{C\equiv N}$	$\Delta\nu_{O-H}$	$\Delta\nu_{S=O}$
1PtZrOX0.3S	3650	1358	3390	1323	2302	260	35
1.5PtZrOZ2.6SB	3651	1379	3237	1327	2305	414	52
1.2PtZrOY3.8S	3646	1400	3244	1340	2307	402	60

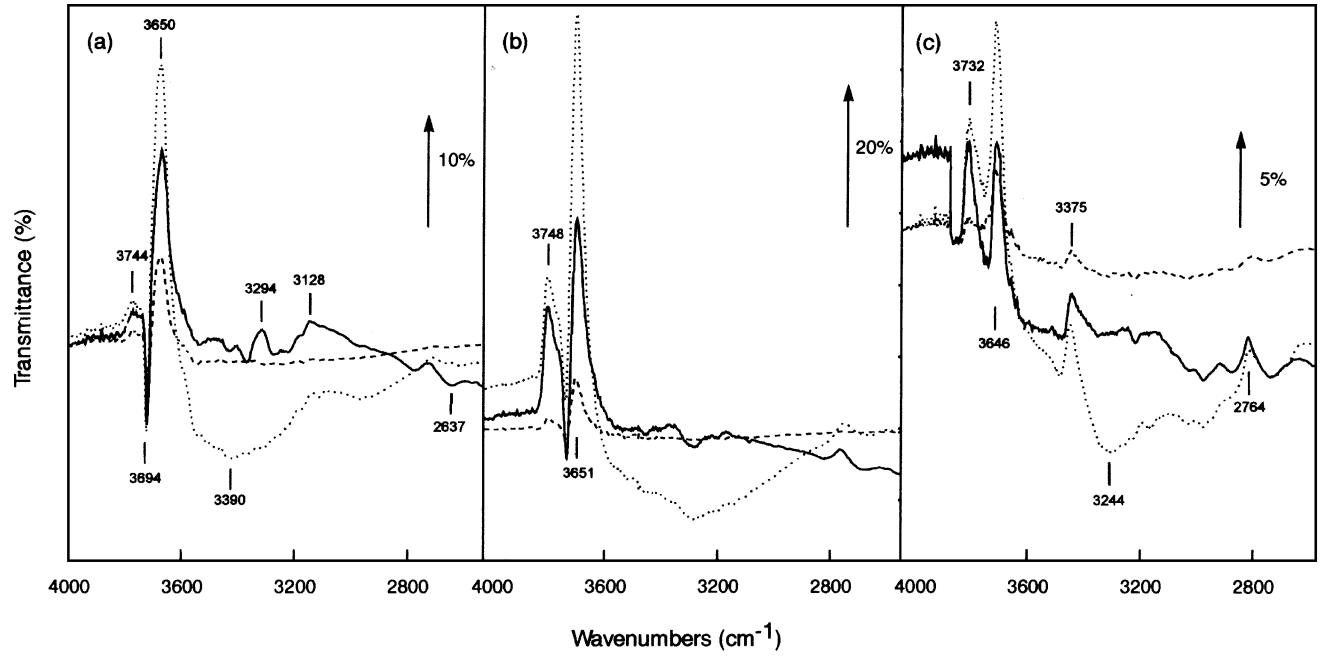

FIG. 10. Difference DRIFT spectra, in the O−H vibration spectral region, expressing the difference between after and before adsorption of CD_3CN on different catalysts: (a) 1PtZrOX0.3S, (b) 1.5PtZrOZ2.6SB, (c) 1.2PtZrOY3.8S. (---) At low coverage, (···) after saturation and desorption at room temperature, (—) after desorption at 373 K.

isomerization proceeds via chain processes limited by hydride transfer steps, hydride transfer being enhanced by the presence of Pt which dissociates molecular hydrogen. Nevertheless, a classical bifunctional mechanism cannot be eliminated. Actually, there is dynamic modification of the surface acid properties of Pt/SZ by hydrogen, where Lewis sites interact with dissociated H atoms to give Brønsted sites (38). Moreover, in the absence of hydrogen these acid

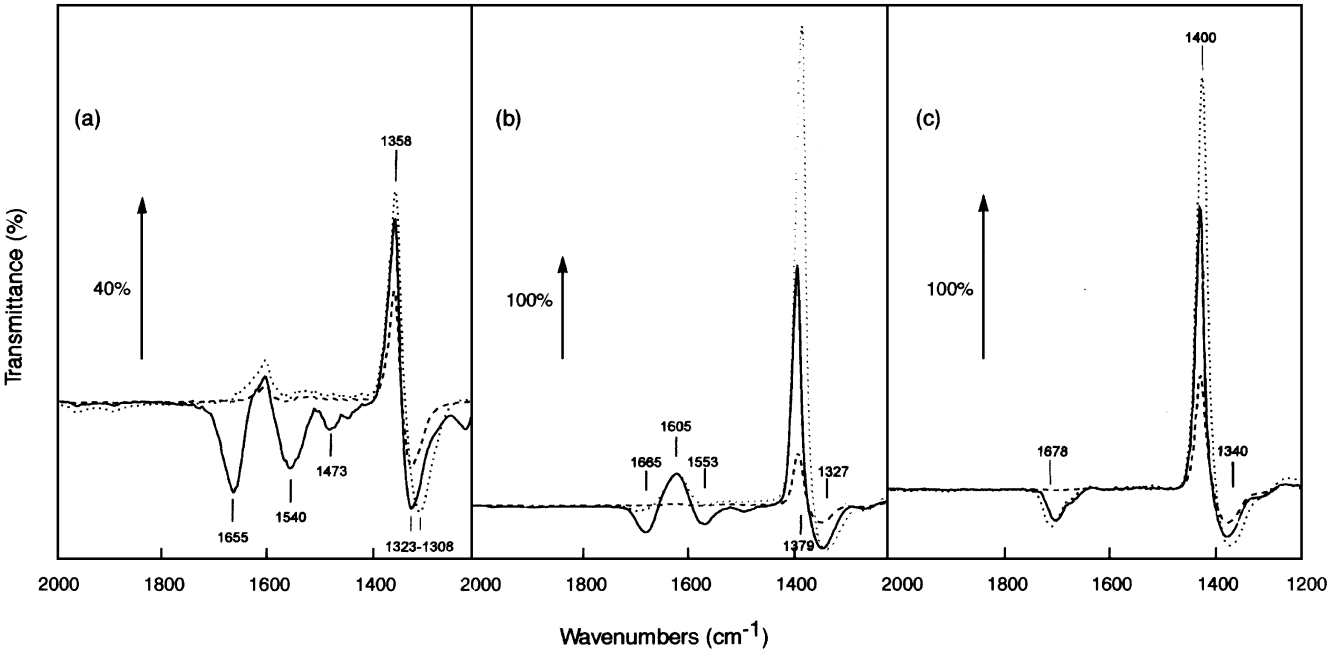

FIG. 11. Difference DRIFT spectra, in the S=O vibration spectral region, expressing the difference between after and before adsorption of CD_3CN on different catalysts: (a) 1PtZrOX0.3S, (b) 1.5PtZrOZ2.6SB, (c) 1.2PtZrOY3.8S. (---) At low coverage, (···) after saturation and desorption at room temperature, (—) after desorption at 373 K.

sites disappear very fast, in agreement with the equilibrium

$$Zr^{4+} + 0.5H_2 \rightleftharpoons Zr^{3+} + H^+$$

proposed by Tichit *et al.* (29). The partial reduction of ZrO_2, for instance, by outgassing at high temperature, does indeed produce Zr^{3+}, identified by ESR by Chen *et al.* (39). In this frame the concentration of Brønsted sites, which are the active species in the classical bifunctional mechanism, increases with H_2 pressure. It is therefore not surprising that the rate increases since the rearrangement of the carbocations on Brønsted sites is rate determining.

2. ROPs, which can be formed by different pathways. A first possibility is the metal-catalyzed hydrogenolysis of endocyclic C–C bonds to nC_7, 2MH and 3MH; however, this reaction is unlikely because (i) no reaction was observed on Pt/Al_2O_3 under atmospheric pressure of H_2 and 650 K, whatever the Pt dispersion (40), and (ii) when the conversion was increased, under isothermal conditions, the ROPs clearly appeared as secondary products. A second possibility is metal-catalyzed hydrogenolysis, not of the cyclohexane ring, but of the cyclopentane ring of product ACPs, which is much easier (41). Finally, a third possible pathway is the endocyclic β-scission of an alkylcyclopentyl ion (22, 23). Although unfavored, this latter pathway cannot be ruled out since at high H_2 pressure (2.5 MPa) their selectivity (5–10%) and formation rate remain the same in the absence and the presence of 70 ppm thiophene (42). Moreover, these compounds were also formed with Pd/SZ, in which Pd is not a good hydrogenolytic metal (42).

The main reaction is the isomerization of MCH to ACPs, which has been thoroughly investigated on zeolites (23). Sulfated zirconia shows in this reaction the same selectivity as ZSM5, despite a mesoporous texture. The reaction has been shown to proceed through the skeletal isomerization of the methylcyclohexyl carbocation formed by protonation of a cyclohexene intermediate, which is an easy reaction. The conversion of MCH is then a good test to characterize the acidity of bifunctional catalysts. As expected, the activity changes with the surface area of the zirconia precursor, the amount of sulfur, and the method of platinum deposition.

The total "number of acid sites," determined by TPD of acetonitrile, is reported in Table 2, as is the fraction of these sites that retain acetonitrile at high temperature. It appears from this table that the efficiency of the sulfate species for the promotion of acidity increases with the surface area of the parent zirconia: for the same standard pretreatment, the average number of sites per S atom increases when the surface area of zirconia increases from 150 to 270 $m^2\ g^{-1}$. The strength of the acid sites, better estimated from the fraction of CH_3CN desorbed under the high-temperature peak, is sensitive to the pretreatment temperature (1.5PtZrOZ2.6SB and –C samples) and to the mode of

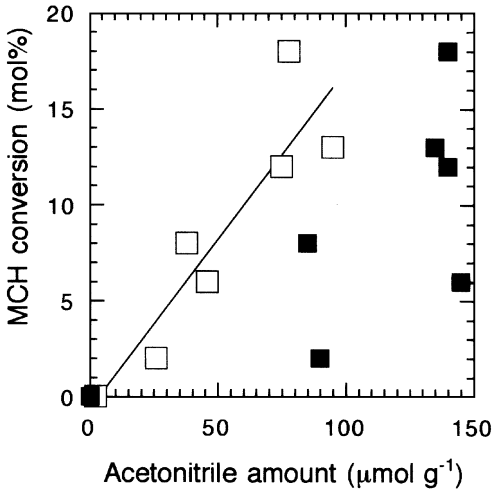

FIG. 12. MCH conversion at 450 K as a function of the total amount of acetonitrile adsorbed (■) and the acetonitrile amount that desorbs at high temperature (□, —) on various Pt/SZ catalysts.

Pt introduction (1.2PtZrOY3.8S and 1.7PtZrOY3.8S samples). The introduction of Pt onto the support clearly reduces the number of acid sites. In this respect, H_2PtCl_6 has a stronger inhibiting effect than $Pt(acac)_2$, since the high-temperature peak of CH_3CN desorption is larger and shifted to higher temperatures (Fig. 4).

When considering all the catalysts for which TPD of CH_3CN has been carried out, a rough correlation is seen to exist between the reactivity at 450 K and the amount of CH_3CN that desorbs at high temperature (Fig. 12). This correlation is much better than when reactivity is considered a function of the total CH_3CN amount desorbed. The most reactive sample, which shows a significant deviation from this correlation, is 1.7PtZrOY3.8S prepared from $Pt(acac)_2$. It is worthy of note that this sample retains a larger fraction of CH_3CN which desorbs at the highest temperature (Fig. 4).

This emphasizes the necessity of identifying, as precisely as possible, the acid properties of the bifunctional catalyst, to understand its catalytic properties. It is interesting to compare the results obtained by the different methods for studying acidity. While TPD of acetonitrile shows clear differences between 1PtZrOX0.3S, 1.5PtZrOZ2.6SB, and 1.2PtZrOY3.8S, for instance, the DRIFTS experiments using the same probe show only small differences in the ν_{CN} vibrations, low values of the ν_{OH} shifts, and noticeable shifts of ν_{SO} vibrations. In previous work on the acidity of sulfated zirconia (28), it was reported that the shift of the band at 3650 cm^{-1} was not representative of the strong acidity of the material, and it was proposed that strong acidity was related to a broad OH band appearing between 2950 and 3250 cm^{-1}. This band was considered characteristic of the protons of HSO_4 species H-bonded to neighboring oxygens. As this band is broader, its shift on adsorption of benzene

could not be observed, and the situation for acetonitrile is probably the same.

The magnitude of the shift of the hydroxyl band at 3650 cm^{-1} on CH_3CN adsorption is comparable to that reported by Adeeva *et al.* (37) for SZ and Fe,Mn–SZ and corresponds approximately to the shift observed with CsHY zeolites, for a solid of low acidity. In contrast, the shift of the same hydroxyl groups resulting from H- bonding with benzene corresponded to an acidity of SZ close to that of HY zeolites (28). This clearly illustrates the fact that acidity is not an intrinsic value and depends on the molecular probe used to characterize it. It can be pointed out that, on acetonitrile adsorption, the ν_{SO} vibration also shifts to higher values which reflect a lower covalency of the S=O bond. The adsorption of ammonia on similar catalysts (29) induced shifts of about 36 cm^{-1} on the sulfate band; therefore it seems that acetonitrile is not a really weak base. Since the acidity of SZ is usually associated with the covalent sulfate bond, that means that acetonitrile interacts strongly with the surface and modifies the solid. The shift of the S=O band is indeed an indicator of the acid strength, and is better related to the amount of CH_3CN desorbing under the high-temperature peak in TPD experiments and catalytic activity for MCH conversion than the shift of OH groups.

It is also interesting that the bifunctional 1.2PtZrOY3.8S catalyst shows catalytic properties similar to those of 1PtZrOS–Fe,Mn for MCH conversion in the presence of hydrogen, as was recently reported for the bifunctional isomerization of *n*-butane (37). In the absence of hydrogen, several authors have found much higher activities for the isomerization of butane on Fe,Mn–SZ (8–10); however, the interpretation of this high activity in terms of superacidity was not confirmed by direct measurements of acidity. To account for this discrepancy, Adeeva *et al.* (37) proposed a greater stabilization of the transition state on Fe,Mn–SZ. An alternative interpretation, based on former work on superacids (43–45) is possible, in view of the fact that the particular properties of Fe,Mn–SZ appear only in the absence of hydrogen. In weak superacids, such as CF_3SO_3H, alkanes without tertiary hydrogen are isomerized very slowly. This lack of reactivity can be overcome by adding olefins to the reaction medium or by the formation of a charge transfer complex by anodic oxidation of the alkane (45). In that case, the isomerization of butane occurs just above room temperature. The formation of olefins is not strictly required, and the following scheme was proposed: $RH \rightarrow RH\cdot^{+} \rightarrow R\cdot + H^{+} \rightarrow R^{+}$. Indeed the bimolecular process of dimerization of the *sec*.-butyl radical to 2,2-dimethylhexane is fast, and the subsequent cracking of dimethylhexane yields isobutane and butyl cations, which can react further. In the case of SZ, the oxidant can be Fe^{3+} or Mn^{4+}, which would be partially reduced in the presence of hydrogen and platinum. The acid strengths of CF_3SO_3H and sulfated zirconia are comparable ($H_0 \approx -14.5$) and can further justify this proposal.

In conclusion, sulfated zirconias could be alternatives to zeolites for the isomerization of naphthenes. This reaction might follow a classical bifunctional mechanism in the presence of platinum where the number of active Brønsted sites increases with H_2 pressure. The addition of platinum noticeably alters the distribution of acid sites of the support, and the method used to introduce Pt is important in that respect. The adsorption of acetonitrile gives reliable information on the number of sites, but, because of the strong interaction with the surface, modifies the solid in such a way that a very pessimistic representation of the stronger acidity is obtained.

ACKNOWLEDGMENTS

The authors gratefully thank Dr. Gordon McDougall and Dr. Ronald Brown (University of Edinburgh, U.K.) for helpful discussion and IR experiments. C.W. thanks Total Raffinage et Distribution for a scholarship.

REFERENCES

1. Holm, V. C. F., and Bailey, G. C., U.S. Patent 3,032,599 (1962).
2. Hino, H., Kobayashi, S., and Arata, K., *J. Am. Chem. Soc.* **101**, 6439 (1979).
3. Yamaguchi, T., and Tanabe, K., *J. Phys. Chem.* **90**, 4794 (1986).
4. Arata, K., *Adv. Catal.* **37**, 165 (1990).
5. Garin, F., Andriamasinoro, D., Abdulsamad, A., and Sommer, J., *J. Catal.* **131**, 199 (1991).
6. Chen, F. R., Coudurier, G., Joly, J.-F., and Védrine, J. C., *J. Catal.* **143**, 616 (1993).
7. Corma, A., Fornés, V., Juan Rajadell, M. I., and López Nieto, J. M., *Appl. Catal. A* **116**, 151 (1994).
8. Hollstein, E. J., Wei, J. T., and Hsu, C. Y., U.S. Patent 4,918,041 (1990); Hollstein, E. J., and Wei, J. T., U.S. Patent 4,956,519 (1990); Hsu, C. Y., and Patel, V. K., U.S. Patent 5,019,571 (1991).
9. Hsu, C. Y., Heibach, C. R., Armes, C. T., and Gates, B. C., *J. Chem. Soc. Chem. Commun.*, 1645 (1992).
10. Jatia, A., Chang, C., MacLeod, J. D., Okubo, T., and Davies, M. E., *Catal. Lett.* **25**, 21 (1994).
11. Cheung, T-K., d'Itri, J. L., Lange, F. C., and Gates, B. C., *Catal. Lett.* **31**, 153 (1995).
12. Zarkalis, A. S., Hsu, C. Y., and Gates, B. C., *Catal. Lett.* **29**, 235 (1994).
13. Cheung, T-K., Lange, F. C., and Gates, B. C., *Catal. Lett.* **34**, 351 (1995).
14. Sommer, J., Hachoumy, M., Garin, F., Barthomeuf, D., and Védrine, J., *J. Am. Chem. Soc.* **117**, 1135 (1995).
15. Adeeeva, V., Lei, G. D., and Sachtler, W. M. H., *Catal. Lett.* **33**, 135 (1995).
16. Liu, H., Adeeva, V., Lei, G. D., and Sachtler, W. M. H., *J. Mol. Catal.* **100**, 35 (1995).
17. Olah, G. A., Prakash, S. K., and Sommer, J., *in* "Super-acids." Wiley, New York, 1985.
18. Weisz, P. B., *Adv. Catal.* **13**, 137 (1962).
19. Hosoi, T., Shimidzu, T., Itoh, S., Baba, S., Takaota, H., Imai, T., and Yokoyama, N., *in* "Symposium on Preparation and Characterization of Catalysts," Preprints, ACS Petroleum Division, Los Angeles Meeting, September 1988, Vol. 33(4), p. 562 (1988).
20. Ebitani, K., Konishi, J., and Hattori, H., *J. Catal.* **130**, 257 (1991).
21. Iglesia, E., Soled, S. T., and Kramer, G. M., *J. Catal.* **144**, 238 (1993).

22. Brouwer, D. M., and Hoogeven, H., *in* "Progress in Physical Organic Chemistry" (R. W. Taft and A. Streitwieser, Jr., Eds.), Vol. 9, p. 179. Interscience, New York, 1972.
23. Weitkamp, J., Jacobs, P., and Ernst, S., *in* "Structure and Reactivity of Modified Zeolites" (P. A. Jacobs, N. I. Jaeger, P. Jírů, V. B. Kazansky, and G. Schulz-Ekloff, Eds.), p. 279. Elsevier, Amsterdam, 1984.
24. Hino, M., Arata, K., and Yabe, K., *Shokubai* **22**, 232 (1980).
25. Saur, O., Bensitel, M., Saad, A. B. M., Lavalley, J. C., Tripp, C. P., and Morrow, B. A., *J. Catal.* **99**, 104 (1986).
26. Morterra, C., Cerrato, G., and Bolis, V., *Catal. Today* **17**, 505 (1993).
27. Nascimento, P., Akratopoulou, C., Oszagyan, M., Coudurier, G., Travers, C., Joly, J. F., and Védrine, J. C., *in* "Proceedings, 10th International Congress on Catalysis, Budapest, 1992" (L. Guczi, F. Solymosi, and P. Tétényi, Eds.), p. 1185. Akadémiai Kiadó, Budapest, 1993.
28. Kustov, L. M., Kazansky, V. B., Figueras, F., and Tichit, D., *J. Catal.* **150**, 143 (1994).
29. Tichit, D., El Alami, D., and Figueras, F., *J. Catal.* **163**, 18 (1996).
30. Coq, B., Walter, C., Brown, R., McDougall, G. S., and Figueras, F., *Catal. Lett.* **39**, 197 (1996).
31. Marshall, P. A., McDougall, G. S., and Hadden, R. A., *Top. Catal.* **1**, 9 (1994).
32. Belloum, M., Travers, Ch., and Bournonville, J. P., *Rev. Inst. Fr. Pet.* **46**, 89 (1991).
33. Chevalier, F., Guisnet, M., and Maurel, R., *C. R. Acad. Sci.* **287**, 3 (1976).
34. Knözinger, H., and Krietenbrink, H., *J. Chem. Soc. Faraday Trans.* **71**, 2421 (1975).
35. Pelminschikov, A. G., van Santen, R. A., Jänchen, J., and Meijer, E., *J. Phys. Chem.* **97**, 11071 (1993).
36. Florian, J., and Kubelková, L., *J. Phys. Chem.* **98**, 8734 (1994).
37. Adeeva, V., de Haan, J. W., Jänchen, J., Lei, G. D., Schünemann, V., van de Ven, L. J. M., Sachtler, W. M. H., and van Santen, R. A., *J. Catal.* **151**, 364 (1995).
38. Ebitani, K., Tsuji, J., Hattori, H., and Kita, H., *J. Catal.* **135**, 609 (1992).
39. Chen, F. R., Coudurier, G., Joly, J-F., and Védrine, J. C., *J. Catal.* **143**, 616 (1993).
40. Walter, C. G., Coq, B., Figuéras, F., and Boulet, M., *Appl. Catal.* **133**, 95 (1995).
41. Zimmer, H., and Paal, Z., *J. Mol. Catal.* **51**, 261 (1981).
42. Walter, C., Ph.D. Thesis, Montpellier, 1995.
43. Germain, A., Ortega, P., and Commeyras, A., *Nouv. J. Chim.* **3**, 415 (1979).
44. Choukroun, H., Germain, A., Brunel, D., and Commeyras, A., *Nouv. J. Chim.* **5**, 39 (1980).
45. Choukroun, H., Germain, A., Brunel, D., and Commeyras, A., *Nouv. J. Chim.* **7**, 83 (1982).